Speed Tracking of an Electric Vehicle Using a Restricted Structure NGMV Control Algorithm *

C. Cebeci, and M. J. Grimble

Abstract — **A Restricted-Structure Non-linear Generalized Minimum Variance (RS-NGMV) algorithm is applied to a scalar quasi Linear Parameter-Varying (qLPV), or State-Dependent (SD), Electric Vehicle speed tracking control problem. The model represents the longitudinal vehicle dynamics with disturbance factors from the road and the environment such as road inclination, aerodynamic drag and the rolling resistance forces. The control problem is based on the longitudinal speed tracking under the impact of these disturbances with an emphasis on the inclination. The simulation studies consider constant speed, UDDS and HWFET drive cycle scenarios as the reference speed profiles. The Restricted-Structure (RS) controller is of low order and uses NGMV optimization to calculate the feedback gains. The results show that RS-NGMV is efficient in dealing with disturbances and parameter variations, and battery State of Charge (SOC) results are also presented.**

I. Introduction

The Minimum Variance (MV) controller was introduced in [1]. It involved the minimization of a cost-function representing the variance of the system's output. Despite its success in some applications, the original MV controller could not be used with non-minimum phase systems and thus the Generalized Minimum Variance (GMV) controller was introduced [2] with additional weighted control term in the cost-function. Later, the NGMV controller was proposed for Non-linear (NL) and time-varying sytems and this was followed by different NGMV control solutions over the years [3].

The RS-NGMV algorithm can use a state-space based Non-linear Generalized Minimum Variance (NGMV) control solution but given a multi-variable Restricted-Structure (RS) controller that is in a low order z-transfer function form within the feedback loop. The aim is to make the controller within the loop have a familiar form for ease of tuning and a classical low order controller such as PID [4,5] may be used. The low-order restricted structure controller has background processing that has a performance similar to the advanced model based NGMV control solution. The restricted structure controller approach is of course not limited to the NGMV design but could use other optimization algorithms like the GPC [6]. However, the NGMV solution is simple to implement and understand.

The RS-NGMV optimal control solutions are derived for Linear-Parameter Varying (LPV) including their special class of quasi Linear-Parameter Varying (qLPV) systems. The LPV modelling has proven to be an effective tool in representing or approximating non-linear systems [7]. If the plant model used by the RS-NGMV is State-Dependent (SD), Linear Time-Invariant (LTI) or Linear Time-Varying (LTV), the optimal control law will be of the same form, except the matrices will be functions of different variables. The RS-NGMV is a model-based control approach thus it is able to adapt to different types of systems. Such model-based techniques are becoming more popular in industry [8] owing to their benefit in using the same controller for different types of system and enabling rapid design and product verification processes.

There is an increasing number of advances in electric vehicles (EVs). The UK Department of Transport announced in 2020 that a historic step would be taken to end the sales of new petrol and diesel cars by 2030 [9]. Such regulatory decisions are also being made by the EU and some states in the USA. Furthermore, major automotive companies have announced going fully electric [10].

This study aims to contribute to the EV problem by considering the impact of disturbances from the road and the environment on the vehicle's performance and the effect on the battery state-of-charge (SOC). The RS-NGMV algorithm is used for the reference longitudinal speed tracking of a Battery/Full Electric Vehicle (referred to as the Electric Vehicle (EV) in the paper.)

The impact of the road grade and environmental disturbances on the EV energy consumption was studied in [11,12] where an online energy consumption prediction algorithm and an energy/fuel saving rule based cruise-control algorithm was based on the road profile determined through GPS data. This study is different in that the control objective prioritizes the speed tracking performance and variations of parameters are included within the model used for design. However, the SOC characteristics are still investigated to analyze the impact of high performance tracking on the battery.

The paper is organized as follows: Chapter 2 shows the longitudinal vehicle dynamics equations and derives the qLPV/SD model. Chapter 3 presents the EV powertrain with its elements and equations. Chapter 4 demonstrates the performance of the RS-NGMV controller. A PI controller is introduced as a baseline design for comparison because it is used for the low-order restricted structure employed by the optimal RS-NGMV controller that is derived. In chapter 5, the simulation results are demonstrated and analyzed. Finally, the conclusions discuss the outputs of the work.

II. QLPV/STATE-DEPENDENT PLANT MODEL

In this chapter, the longitudinal vehicle dynamics are introduced and represented in qLPV or SD form.

* C. Cebeci would like to thank the Turkish Ministry of National Education for the sponsorship of his postgraduate studies.

Authors are with the Electronics and Electrical Dept., University of Strahclyde, Glasgow, UK G1 2TB (e-mail: cagatay.cebeci@ strath.ac.uk).

This is a peer-reviewed, accepted author manuscript of the following article: Cebeci, C., & Grimble, M. (2022). Speed tracking of an electric vehicle using a restricted structure NGMV control algorithm. In 2022 European Control Conference, ECC 2022 (pp. 790-795). (2022 European Control Conference, ECC 2022). IEEE. https://doi.org/10.23919/ECC55457.2022.9838220

longitudinal dynamics and the powertrain components of the EV in this study are based on [13-16].

A. Longitudinal Vehicle Dynamics

The longitudinal vehicle dynamics follow from Newton's second law of motion and are defined by the summary of physical forces in action, that is,

$$F_{total} = ma = F_x - F_{grade} - F_{aero} - F_{roll} \quad (1)$$

where m is the mass of the vehicle and a stands for the acceleration which is the derivative of the longitudinal velocity V_x. The longitudinal forces in (1) are described below.

- Tractive force enables the traction of the vehicle:

$$F_x = (\tau_{motor} - \tau_{loss})\frac{G}{r_w} - F_{br}, \quad (2)$$

where motor torque and torque losses are given by, τ_{motor} and τ_{loss}. The terms G and r_w denote the gear ratio and wheel radius, respectively. Finally, the notation, F_{br}, represents the braking force.

- Road grade force:

$$F_{grade} = mgsin\theta = mg\theta. \quad (3)$$

Since the roads are designed to relatively small inclinations, F_{grade} can be linearized at inclination angle $\theta = 0$ and hence $sin\theta = \theta$.

- Aero dynamic drag force:

$$F_{aero} = \frac{\rho AC_d}{2}(V_x + V_{wind})^2 = \frac{\rho AC_d}{2}V_x^2. \quad (4)$$

For this study, it is assumed that $V_{wind} = 0$. The parameters ρ, A and C_d are the mass density of air, vehicle frontal area and drag coefficient, respectively.

- Rolling resistance or rolling friction force:

$$F_{roll} = mgC_r, \quad (5)$$

where C_r is the rolling resistance coefficient.

The qLPV/SD model is extracted by using (1) - (5). The state-space model uses the state $x(t) = V_x(t)$ where $\dot{x}(t) = a(t)$,

$$\dot{x}(t) = -\frac{\rho AC_d V_x(t)}{2}x(t) + \frac{1}{m}F_x(t) - g\theta(t) - gC_r, \quad (6)$$

$$y(t) = x(t) + W_d, \quad (7)$$

where the force $F_x(t)$ is the net input that is responsible from the vehicle's traction, $y(t)$ is the output (longitudinal velocity) and W_d is the output disturbance. The model above represents the original non-linear system within a linear form. For the SD modelling the above representation would be sufficient, while the qLPV may also include scheduling parameters that are exogenous to the model and time-varying. For example, the scheduling parameters may be chosen as below,

$$p = (p_1, p_2) = \left(-\frac{\rho AC_d}{2}, \frac{1}{m}\right). \quad (8)$$

For further details on the qLPV/SD models, there are many references including [3,7].

III. EV POWERTRAIN MODELS AND EQUATIONS

The EV powertrain contains a Lithium-Ion (Li-Ion) battery as the source of energy, an AC electric motor to produce torque for traction, regenerative brake system and the driveline. Note that the EV components of section III are not represented in the state-space model given in section II. However, all of these components help determine the tractive force F_x. To clarify how this works, in the actual Simulink model, the controllers (both PI and RS-NGMV) produce acceleration or deceleration commands that are received by the electric motor and the brake system. Then, through the driveline the tractive force F_x is calculated as shown in (2). From this perspective, it can be seen that the qLPV/SD model derived in (6) and (7) is an approximation of the full EV model.

A. Battery Equations

The Li-Ion battery is modelled using a basic Equivalent Circuit Model (ECM) [16]. The ECM consists of an open-circuit voltage (OCV) denoted by V_{oc}, an internal resistance R_{in} in series to accessory load R_{load}. The battery current is given by,

$$I = \frac{V_{oc} - \sqrt{V_{oc}^2 - 4R_{in}P_{motor}}}{2R_{in}}, \quad (9)$$

where P_{motor} is the motor power combined with the accessory load (AC, multi-media and etc.). The battery power is then calculated considering the dissipative losses,

$$P_{batt.} = IV_{oc} - I^2R_{in}. \quad (10)$$

The battery SOC is given an initial value $z(0) = 0.95$ (95%) at the start of the vehicle journey and then updated by,

$$z(t) = z(t-1) - \frac{IT_s}{Q}, \quad (11)$$

where T_s is the sampling time, and, Q is the energy capacity of the battery.

B. Electric Motor

The electric motor output power, P_{motor}, equals to the input power minus the motor losses,

$$P_{motor} = P_{in} - P_{loss} = \tau_{motor}\omega_{motor} - (C + k_c\tau^2 + k_i\omega + k_\omega\omega^3), \quad (12)$$

where the input power is the product of motor torque, τ_{motor}, and rotational speed of the shaft, ω_{motor}, and the losses are a combination of these with some motor constants C, k_c, k_i, k_ω. All of the mentioned parameters are assumed known and measureable.

C. Driveline

The type of traction in this model is of the forward wheel drive (FWD) where the EV driveline is the final stage before the power is delivered to the wheels.

IV. RS-NGMV CONTROL

This chapter starts with the state-space representation of the entire system in an augmented system form. Next, the baseline scalar PI controller [18] is represented in a restricted structure form. Then, optimal RS-NGMV control law is introduced.

A Augmented State-Space System

The full form of a qLPV system matrix is represented in the form, $A(x(t), u(t), p(t))$, but in this paper it is denoted as A_t.

Consider the subsystems below:

- The linear plant subsystem which can be LPV, qLPV, SD, LTV or simply LTI. Recall the qLPV plant from (6) and (7), and represent in state-space terms (discretized),

$$x_0(t+1) = A_{0t}x_0(t) + B_{0t}u_0(t-k), \quad (13)$$

$$y(t) = C_{0t}x_0(t) + D_{0t}u_0(t-k), \quad (14)$$

  where k denotes the predictive steps characteristic to the NGMV controllers.

- The disturbance subsystem:

$$x_d(t+1) = A_{dt}x_d(t) + D_{dt}\omega(t), \quad (15)$$

$$y_d(t) = C_{dt}x_d(t), \quad (16)$$

  where matrices are also used to obtain the output disturbance model $W_d = C_{dt}(zI - A_{dt})^{-1}D_{dt}$. See Table 1 for the model used in this study.

- The error weighting subsystem:

$$x_p(t+1) = A_{pt}x_p(t) + B_{pt}e(t), \quad (17)$$

$$y_p(t) = C_{pt}x_p(t) + D_{pt}e(t), \quad (18)$$

  where $e(t) = r(t) - z(t)$ is the reference tracking error signal. The matrices in (17) and (18) are extracted from the cost-function error weighting $P_c(t)$ which is in transfer-function form. The product of the error signal and the weighting term is the weighted error signal,

$$e_p(t) = d_p(t) + C_{pt}x(t) + E_{pt}u(t-k) \quad (19)$$

- The input subsystem:

$$x_u(t+1) = A_{ut}x_u(t) + B_{ut}u_0(t-k), \quad (20)$$

$$y_u(t) = C_{ut}x_u(t) + D_{ut}u_0(t-k), \quad (21)$$

  can be non-linear and $u_0(t) = z^{-k}(W_{1k}u)t$. For this paper, the assumption is $W_{1k} = I$ because the controller does not include non-linearities.

Let $x(t) = \left(x_0(t), x_d(t), x_p(t), x_u(t)\right)^T$ and augment the subsystems in (12-20) under the state-space representation,

$$x(t+1) = A_t x(t) + B_t u_0(t-k) + D_t\xi(t) + d_d(t), \quad (22)$$

$$y(t) = C_t x(t) + E_t u_0(t-k) + d(t), \quad (23)$$

where $\xi(t)$ is the stochastic component of the input disturbance, $d_d(t)$ is the known input disturbance signals and $d(t)$ is the vector of known output disturbances. The output (23) is not measureable but is controlled. The measureable output is given by,

$$y_m(t) = C_{mt}x(t) + E_{mt}u_0(t-k) + d_m(t), \quad (24)$$

and the observations signal $z(t) = v(t) + y_m(t)$. For more details on the augmented system derivation, refer to [3,4].

B. Baseline PI Controller

The scalar PI controller that serves as the baseline method for the RS-NGMV is formulated as below,

$$u_{PI}(t) = k_p e(t) - \frac{1}{1-z^{-1}}k_I T_s e(t), \quad (25)$$

where k_p and k_I are proportional and the integral gains respectively. The reference signal $r(t)$ is either constant speed for cruise control or the drive cycle profile UDDS/HWFET and z(t) being the observations signal.

The PI controller in (25) can be expressed in the RS form,

$$u_{RS-PI}(t) = f_1(z^{-1})k_p e(t) - f_2(z^{-1})k_I T_s e(t), \quad (26)$$

with the functions $f_1(z^{-1}) = 1$ and $f_2(z^{-1}) = 1/(1-z^{-1})$. Defining the function terms in the vector $F_e(t) = [f_1,\ f_2]^T e(t)$ and the gains in the vector $\bar{k}_c = \left[k_p,\ k_I T_s\right]^T$, the scalar RS-PI can be parameterized as:

$$u_{RS-PI}(t) = F_e(t)\bar{k}_c. \quad (27)$$

C. RS-NGMV Controller

The RS-NGMV control structure for this study is presented in Fig. 1. The controller is a special case, referred to as the parallel form RS-NGMV [4,5], which is useful if a low-order controller that already stabilizes the system is available. The parallel form control input signal is a combination of fixed gain RS-PI given in (27) and the gain deviations component,

$$u_{RS-NGMV}(t) = F_e(t)\bar{k}_c + F_e(t)\tilde{k}_c(t). \quad (28)$$

The deviations $\tilde{k}_c(t)$ are calculated by the RS-NGMV optimization procedure which uses an LPV Kalman filter and they are used to update the total gain, $k_c(t) = \bar{k}_c + \tilde{k}_c(t)$, continuously. This becomes constant in the steady-state when disturbances are absent.

The LPV Kalman filter (LPVKF) is of the predictor-corrector type [19] and is used for calculating the optimized feedback control gains. This allows the controller to adapt to the parameter variations and set-point changes rapidly. By using (22) iteratively, the k-steps ahead predictor is obtained,

$$\hat{x}(t+k|t) = A_t^k\hat{x}(t|t) + \sum_{j=1}^{k} A_{t+j}^{k-j}B_{t-j-1}u_0(t+j-1-k) + d_{dd}(t+k-1). \quad (29)$$

The prediction errors are calculated in a similar way to (29),

$$\hat{e}(t+k|t) = d_p(t+k) + C_{pt+k}\hat{x}(t+k|t) + E_{pt+k}u_0(t). \quad (30)$$

The disturbance terms of the predictor model are known and deterministic. The d_p is the known output disturbance signal.

With the augmented system, the LPVKF and the restricted structure defined, the RS-NGMV control law can be derived. Let the RS-NGMV optimal control cost function be defined as,

$$J = E\{\emptyset_p^T(t+k)\emptyset_p(t+k)\}, \quad (31)$$

the minimization of which will return the controller. The cost function J is the variance of the pseudo output signal $\emptyset_p$,

$$\emptyset_p(t+k) = P_p(t)e_p(t+k) + F_{c0}u_0(t) + F_{c1}\tilde{k}_c(t) + F_{c2}\Delta\tilde{k}_c(t) + F_e^T(t)(F_{ck}u)(t). \quad (32)$$

The terms in (32) are error and control weightings:

- Tracking error weighting: $P_p(t) = F_e^T(t)E_{pt+k}^T\lambda_p^2$,
- Control weightings: $F_{c0} = F_e^T(t)\lambda_u^2$, $F_{c1} = \lambda_k^2$ and $F_{c2} = \lambda_d^2$. These represent the control input weighting, controller gain deviation weighting and weightings on the increments on the gain deviations.
- The term F_{ck} is the control weighting operator and is assumed to be full rank and invertible.

In summary, the solution of (31) involves algebraic manipulations that include substitution of some terms, defining new matrices or vectors and finally computing the gradient. The condition of optimality is determined by setting the gradient to zero. The controller gain that minimizes the cost function,

$$k_c(t) = -X_0(t)^{-1}(P_p(t)d_{pd}^0(t+k) + \varphi_k(t)), \quad (33)$$

where new terms are defined as:

- $\varphi_k(t) = -\lambda_k^2 k_c - \lambda_d^2 k_c(t-1)$,
- $d_{pd}^0(t+k) = d_p(t+k) + C_{pt+k}d_{dd}(t+k-1) + C_{pt+k}\hat{x}(t+k|t)$
- $X_0(t) = F_e^T(t)\left(F_{ck} + E_{pt+k}^T\lambda_p^2E_{pt+k}\right)F_e(t) + \lambda_k^2 + \lambda_d^2$.

V. Simulation Results

The controller parameters used for the simulation studies are given in Table 1 under the Appendix. The qLPV/SD model in (6) and (7) is discretized for sampling time $T_s = 1s$ using the Euler technique. The EV parameters are selected from [16,18], the first of which uses the pre-release speculated parameters of Chevrolet Volt Gen I. The simulations are performed using Matlab/Simulink and the NGMV toolbox of the ISC Ltd.

A. Speed Tracking Results

The tracking performance is displayed in Fig. 2 to Fig. 7. In Fig. 2 and 3, the EV set-point is constant speed for cruise-control with the initial value set to zero. The acceleration is modelled as a 1st order transfer-function with approximated acceleration characteristics of the passenger car. In Fig. 2, the flat road $\theta(t) = 0$ and in Fig. 3, the $\theta(t) = 0.1\sin(2\pi ft)$, represents a hilly route, where $f = 0.005Hz$ and 0.1 refers to 10% road grade (or 5.74 degrees). For the first case, the RS-NGMV shows faster settling time and less overshoot. For the latter, the variations in the road grade disturbance is clearly visible on the PI controller's response. On the other hand, RS-NGMV does not indicate any negative effects.

In the Figures 4-7, the road grade is based on the same hilly route profile that was mentioned earlier. The Fig. 4 and 5 demonstrate, the tracking results with Urban Dynamometer Driving Schedule (UDDS) as the reference drive-cycle, divided as first and second halves, respectively, for illustrative purposes. Similarly, the RS-NGMV controller shows high performance while the PI controller struggles with the frequent acceleration/decelerations, stops and the road-grade. The Fig. 6 and 7, shows the reference tracking performance for the Highway Fuel Economy Test (HWFET) drive-cycle and the observations on the results are similar to the UDDS case. Note that the official lengths given for the UDDS and HWFET cycles, are 1369 seconds and 765 seconds, respectively.

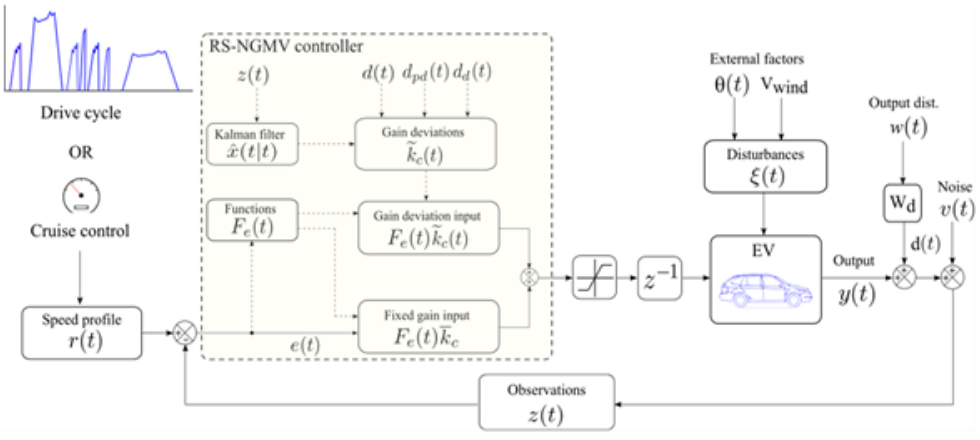

Figure 1. RS-NGMV control diagram.

To further support the results, consider the RMS value of the reference speed tracking errors as given by the,

$$RMS(e(t)) = \sqrt{\frac{1}{T}\int_{t-T}^{t} e(\tau)^2 d\tau}, \quad (34)$$

calculations of which returns as the values below for each case,

- $RMS(e_{RS-NGMV}, e_{PI}) \cong (0.79, 1.21)$ for UDDS,
- $RMS(e_{RS-NGMV}, e_{PI}) \cong (0.40, 0.82)$ for HWFET,

Showing RS-NGMV can have up to 50% less tracking errors.

B. Battery SOC Results

The battery SOC results for the UDDS and HWFET drive-cycles shown previously are illustrated in the Fig. 8 and 9. The initial battery SOC is 95% and it is shown how the SOC changes over the drive cycles. Naturally, the general trend is decreasing but there are also times when regenerative braking is active and some energy is recovered which increases the SOC. In both cases, the final SOC value of the RS-NGMV is slightly lower than that of the PI's. The reason is the control effort of the RS-NGMV increasing in the presence of the disturbances to mitigate their affects. However, the difference is very minimal. Including the other runs, the difference is observed to appear in the margin of $z_{RS-NGMV} - z_{PI} \leq 0.05$.

Assessing the overall tracking performance, it may appear as the variations caused by the disturbances are not too large to cause issues. However, in the real world applications it is expected that even the small speed variations could impact the passenger comfort badly thus keeping the drive as smooth as possible would greatly improve the quality. Furthermore, the purpose of RS-NGMV is to provide an advanced control solution in a low order control structure like the PI here. This is the reason why PI has been chosen for comparison because it's the baseline controller for the RS-NGMV.

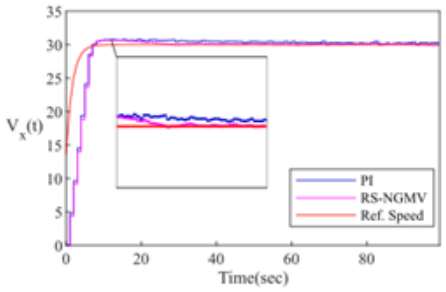

Figure 2. Cruise Control for $\theta(t) = 0$

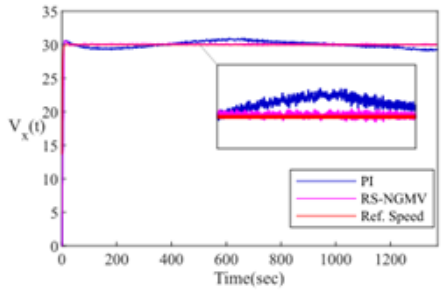

Figure 3. Cruise Control for $\theta(t) = 0.1\sin(2\pi ft)$

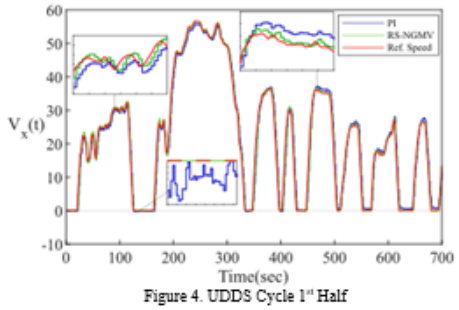

Figure 4. UDDS Cycle 1st Half

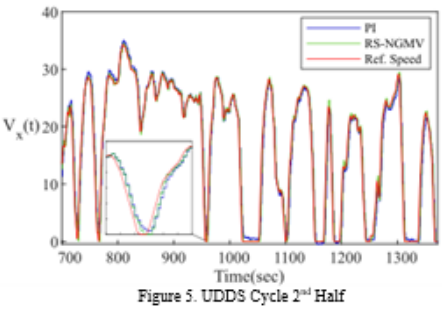

Figure 5. UDDS Cycle 2nd Half

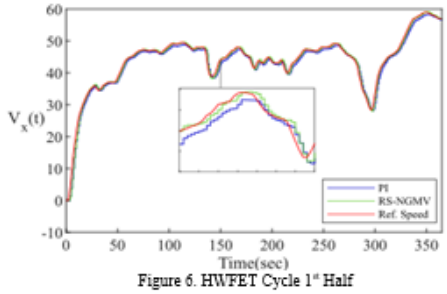

Figure 6. HWFET Cycle 1st Half

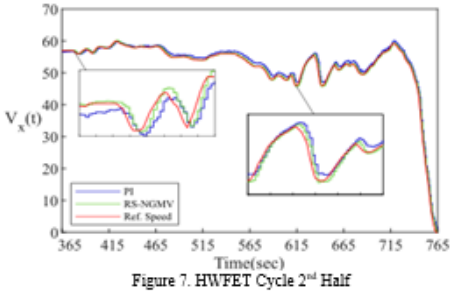

Figure 7. HWFET Cycle 2nd Half

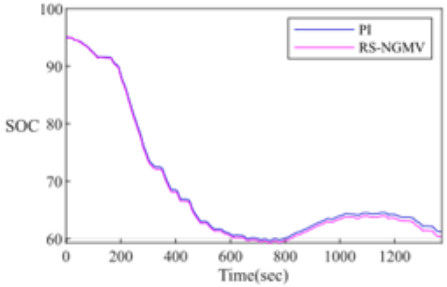

Figure 8. UDDS Battery SOC

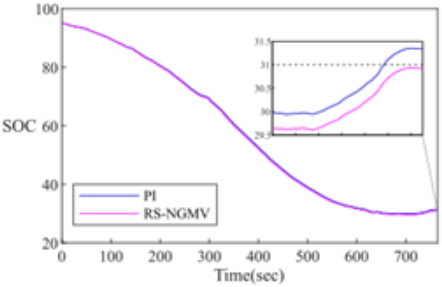

Figure 9. HWFET Battery SOC

C. EV Range Estimations

As the final set of results, the EV range estimations for the UDDS and HWFET drive cycles are presented. To further demonstrate the impact of the road-grade disturbance, we consider both $\theta(t) = 0$ and varying $\theta(t) = 0.1\sin(2\pi ft)$, once again. Firstly, define the change of position,

$$\Delta q = V_x T_s = q(t) - q(t-1) \tag{35}$$

between the two time instants previous and present. Using (35) the position of the vehicle is calculated and updated.

The estimated EV range is extrapolated from the driving cycle information, that is, the total distance travelled and the depletion of the battery SOC [16]. The estimate is given by,

$$\hat{q} = q_{total}(z_{max} - z_{min})/(z(0) - z(\infty)) \tag{36}$$

where q_{total} is the total distance travelled, z_{max} and z_{min} are the SOC limits, $z(0)$ and $z(\infty)$ are the initial and final SOC values. The results for each drive-cycle and road-grade are:

- $(\hat{q}_{RS-NGMV}, \hat{q}_{PI}) \cong (40.09mi, 41.79mi)$ for $\theta(t) = 0$
- $(\hat{q}_{RS-NGMV}, \hat{q}_{PI}) \cong (13.43mi, 13.61mi)$ for $\theta(t)$ var.
- $(\hat{q}_{RS-NGMV}, \hat{q}_{PI}) \cong (47.28mi, 47.94mi)$ for $\theta(t) = 0$
- $(\hat{q}_{RS-NGMV}, \hat{q}_{PI}) \cong (14.67mi, 14.75mi)$ for $\theta(t)$ var.

The disturbances reduce the range to roughly $1/3$ of the standard. It also indicates the importance of correct SOC information when planning a journey.

VI. Conclusion

In this study, the tracking performance was prioritized but the RS-NGMV cost-function can be modified or re-tuned to compromise the performance to preserve the battery SOC. For the purposes of this study, it was sufficient to assume that the initial battery SOC starts at 95% and to use the basic ECM battery model. The RS-NGMV can be used for the SOC estimation and control of battery charging problems. The future work will thus extend around the battery topics using advanced ECMs [20] or physics-based models [21].

Appendix

The controller parameters are given in Table 1.

TABLE I. RS-NGMV and PI controller parameters

Weights	***Symbol***	***Value***
Dynamic error	λ_p	1
Cost-function error	P_c	$1000\frac{1-0.97z^{-1}}{1-z^{-1}}$
Cost-function control	F_{ck}	$\mathbf{0.001}\frac{\mathbf{1-z^{-1}}}{\mathbf{1-0.1z^{-1}}}$
Output disturbance model	W_d	$\frac{\mathbf{0.1z^{-1}}}{\mathbf{1-0.98z^{-1}}}$
Control input	λ_u	0.0001
Gain deviation	λ_k	diag(1, 0.1, 0.01)
Deviation increments	λ_d	diag(100, 50, 0)
Proportional gain	k_p	15
Integral gain	k_I	0.25

Acknowledgement

We are grateful for our discussions with Dr. Luca Cavanini and Dr. Pawel Majecki of the ISC Ltd.

References

[1] K. J. Åström, Introduction to Stochastic Control Theory, Academic Press, 1970.

[2] P. Wellstead and M. Zarrop, Self-Tuning Systems: Control and Signal Processing, Wiley, 1991.

[3] M. Grimble, P. Majecki, Nonlinear Industrial Control Systems, Springer, 1st edition, 2020.

[4] M.J. Grimble, "Reduced-Order Non-Linear Generalised Minimum Variance Control for Quasi-Linear Parameter Varying Systems," IET Control Theory and Applications, vol. 12, issue 18, pp. 2495-2506, 2018.

[5] C. Cebeci, M.J. Grimble, R. Katebi and L.F. Recalde, "Restricted Structure Non-Linear Generalized Minimum Variance Control of a 2-Link Robot Arm," UKACC 12th International Conference on Control, pp. 367-372, Sheffield, UK, 2018.

[6] M.J. Grimble, P. Majecki, "Restricted Structure Predictive Control for Linear and Non-linear Systems," Int. Journal of Control, 2018.

[7] C. Hoffmann, H. Werner, "A Survey of Linear Parameter-Varying Control Applications Validated by Experiments or High-Fidelity Simulations," IEEE Transactions on Control Syst. Tech., vol. 23, no 2, pp. 416–433, 2015.

[8] H. Ito. Toyota Front-Loads Development of Engine Control Systems Using Comprehensive Engine Models and SIL. (2019). [Online]. Available: https://uk.mathworks.com/company/user_stories/reducing-time-to-market-using-model-based-design-qa-with-toyota.html

[9] Dept. for Transport, Office for Low Emission Vehicles, Dept. for Business, Energy & Industrial Strategy, The Rt H. A. Sharma MP, and The Rt. H. G. Shapps MP. Government Takes Historic Step Towards Net-zero with End of Sale of New Petrol and Diesel Cars by 2030. (Nov. 18, 2020). Accessed on: Mar. 1, 2021. [Online]. Available: https://www.gov.uk/government/news/government-takes-historic-steptowards-net-zero-with-end-of-sale-of-new-petrol-and-diesel-cars-by-2030.

[10] P.A. Eisenstein, NBC news. GM to Go All-electric by 2035, Phase out Gas and Diesel Engines. (Jan. 29, 2021). Accessed on: Mar. 1, 2021. [Online]. Available: https://www.nbcnews.com/business/autos/gm-go-allelectric-2035-phase-out-gas-diesel-engines-n1256055.

[11] J. Wang, I. Besselink and H. Nijmeijer, "Online Prediction of Battery Electric Vehicle Energy Consumption," EVS 29 Symposium, 2016.

[12] B.Kim, Y.Kim, T.Kim, Y. Park and S.W. Cha, "HEV Cruise Control Strategy on GPS (Navigation) Information," EVS 24 Symposium, 2009.

[13] T. D. Gillespie, Fundamentals of Vehicle Dynamics, SAE Inc., 1992.

[14] Z. Sun, G. G. Zhu, Design and Control of Automotive Propulsion Systems, CRC Press, 2015.

[15] B. Zhang, C. C. Mi and M. Zhang, "Charge Depleting Control Strategies
and Fuel Optimization of Blended-mode Plug-in Hybrid Electric Vehicles," IEEE Trans. on Vehicular Technology, 2011.

[16] G. L. Plett, Battery Management Systems, Volume II: Equivalent-Circuit Methods, Artech House, 2016, vol.2, ch. 3.

[17] Max Pixel. Automobile Design Plan Blueprint Drawing Technical. (2021). [Online]. Available: https://www.maxpixel.net/Automobile-Design-Plan-Blueprint-Drawing-Technical-30577.

[18] MathWorks Student Competitions Team. MATLAB and Simulink Racing Lounge: Vehicle Modeling. (2021). Accessed on: Jan. 12, 2021.
https://github.com/mathworks/vehiclemodeling/releases/tag/v4.1.1.

[19] M. Grimble, M. Johnson, Optimal Control and Stochastic Estimation, Volume I and II, John Wiley, London, 1988.

[20] G. L. Plett, "Extended Kalman filtering for battery management systems of LiPB-based HEV battery packs Part 3. State and parameter estimation," Journal of Power Sources, 2004.

[21] G. Florentino and M.S. Trimboli, "Lithium-ion Battery Management Using Physics-based Model Predictive Control and DC-DC Converters," IEEE Transportation Electrification Conference and Expo (ITEC), 2018.